ACS OMEGA

http://pubs.acs.org/journal/acsodf

Article

Stretchable and Flexible Micro−Nano Substrates for SERS Detection of Organic Dyes

Yuanhang Tan, Kang Yang, Xuefei Zhang,* Ziyu Zhou, Yiting Xu, Atian Xie, and Changguo Xue*

Cite This: *ACS Omega* 2023, 8, 14541−14548

Read Online

ACCESS | Metrics & More | Article Recommendations

ABSTRACT: Surface-enhanced Raman spectroscopy (SERS) is a precise and noninvasive analytical technique to identify vibrational fingerprints of trace analytes with sensitivity down to the single-molecule level. However, substrates can influence this capability, and current SERS techniques lack uniform, reproducible, and stable substrates to control plasma hot spots over a wide spectral range. Herein, we demonstrate a flexible SERS substrate via longitudinal stretching of a polydimethylsiloxane (PDMS) film. This substrate, after stretching and shrinking, exhibits an irregular wrinkled structure with abundant gaps and grooves that function as hot spots, thereby improving the hydrophobic properties of the material. To investigate the enhancement effect of Raman signals, silver nanoparticles (AgNPs) were mixed with Rhodamine 6G (R6G) solution, and the obtained blend was dropped onto the PDMS film to form a coffee ring pattern. According to the results, the hydrophobicity of the substrate increases with the degree of PDMS stretching, achieving the optimal level at 150% stretching. Moreover, the increase in hydrophobicity makes the measured molecules more aggregated, which enhances the Raman signal. The stretching and shrinkage of the PDMS film lead to a much higher density of nanogaps among nanoparticles and nanogrooves, which serve as multiple hot spots. Being highly localized regions of intense local fields, these hot spots make a significant contribution to SERS performance, improving the sensitivity and reproducibility of the method. In particular, the relative standard deviation (RSD) was found to be 2.5544%, and the detection limit was 1×10^{-7} M. Therefore, SERS using stretchable and flexible micro−nano substrates is a promising way for detecting dyes in wastewater.

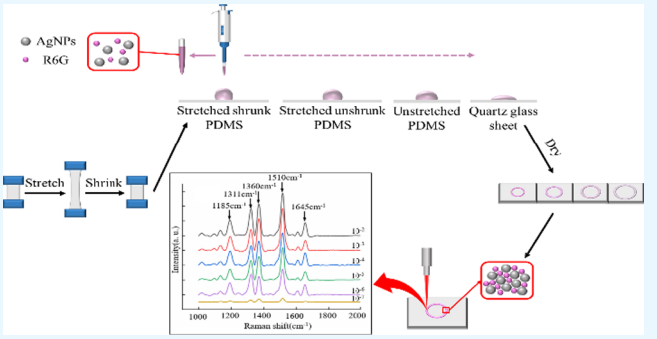

1. INTRODUCTION

Surface-enhanced Raman spectroscopy (SERS) is one of the most powerful techniques in bioanalysis, which benefits from the molecular "fingerprints" of conventional Raman spectroscopy and the enormous enhancement of the signal by plasma nanomaterials (down to the single-molecule level).[1−5] The intensity of the Raman scattering signal absorbed on a rough metal surface is a million times stronger than that generated by an unabsorbed analyte molecule.[6−8] Compared with traditional chromatographic and spectroscopic tools, SERS possesses high sensitivity, nondestructivity, high molecular specificity, fingerprint recognition, and single molecule detection.[9−17] These advantages make SERS suitable for various applications, including bioassays, biomolecular testing, and clinical diagnostics.[18−22] Besides, SERS has good prospects in detecting organic dyes.[23−25]

However, the use of SERS is often influenced by the unique structure of the substrate. SERS substrates are commonly made of metallic nanomaterials that form plasma hot spots to amplify the excitation and emission radiation.[26] Meanwhile, the production of conventional rigid supporting SERS substrates is laborious and time-consuming, often lacking biocompatibility and requiring high raw material and fabrication costs.[26,27] These issues affect the flexibility and conformability of SERS substrates for sensing applications toward complex surfaces in practice.[28] Therefore, flexible substrates have been gradually explored as SERS platforms.[29] SERS substrates composed of flexible and stretchable materials, such as polyethylene terephthalate (PET), polydimethylsiloxane (PDMS),[30] and sodium carboxymethyl cellulose (NaCMC),[31] are advantageous in terms of mechanical flexibility and stretchability[28,32−34] but also possess stability, flexibility, and cost-effectiveness along with high optical transparency[35] and easy preparability.

The formation of wrinkle structures on flexible substrates is an effective way to improve SERS performance. Traditionally,

Received: January 10, 2023
Accepted: March 31, 2023
Published: April 11, 2023

e-beam lithography[36] and reactive ion etching[37] have been used to prepare SERS substrates with wrinkled structures, but these methods are complex and expensive.[38] In turn, mechanical stretching/release has been considered a simple and effective approach, which can transform the two-dimensional flat films into three-dimensional ones along with multiple nanostructures as effective plasmonic substrates.[39] When plasmonic nanostructures are embedded in wrinkled structures, a tightly packed nanostructure array can be produced, resulting in the generation and enhancement of strong electromagnetic fields upon light irradiation.[28,39,40] Along with the formation of wrinkled structures, the material surface induces the emergence of nanogaps and V-shaped nanogrooves, which resemble nanocavities to converge the incident photons and function as plenty of hot spots.[41]

In addition, the formation of wrinkle structures can also change the hydrophobic properties of the material, which is also one of the factors affecting the effectiveness of SERS. In particular, materials with good hydrophilic properties easily absorb the sample solution, which randomly spreads over a large area of the surface and thus reduces the Raman signal.[42] On the contrary, the hydrophobic compounds can effectively accumulate the molecules to be detected within a unit area, thereby enhancing the Raman signal and improving the substrate's detection sensitivity for low-concentration solutions.[43,44] In that regard, flexible materials with hydrophobic properties are selected as the substrates and stretched to increase their surface roughness. This enhances the degree of hydrophobicity, making the substrate more effective in aggregating the detectable substance molecules and further amplifying the SERS effect.

In this study, silver nanoparticles (AgNPs) were synthesized through the Lee−Meisel method using sodium citrate as the reducing and stabilizing agent. The nanoparticles were mixed with Rhodamine 6G (R6G) to achieve the coffee ring[45] pattern for investigating the enhanced Raman signal. The substrate hydrophobicity was changed by the formation of a wrinkled surface structure by stretching the PDMS film to explore the effect of the substrate on the Raman signal. A simple and cost-effective technique, consisting in stretching PDMS films to accomplish the purpose of this study, is expected to open up new prospects for reliable in situ SERS detection of trace organic pollutants in the ecological environment.

2. RESULTS AND DISCUSSION

2.1. Characterization of AgNPs. The gray−green AgNPs were prepared via the Lee−Meisel method using sodium citrate as the reducing and stabilizing agent. Figure 1 displays the UV−vis spectra of the prepared AgNPs, revealing the surface ion absorption peak at 445 nm. The large width of this peak indicated the presence of coarse AgNPs and their wide distribution in the solution. To explore the stability of nanoparticles, the AgNPs were stored in brown glass vials and then in a cool place. After 15 days, they were re-exposed to UV−vis spectroscopic analysis, revealing no significant changes in the spectrogram, which indicated that the products had good stability.

2.2. Transmission Electron Microscopy of AgNPs. To confirm the synthesis of AgNPs and observe their shapes, transmission electron microscopy (TEM) was conducted. The results in Figure 2 depict that the AgNPs had various shapes, spherical, triangular, rod-shaped, etc. The TEM image indicated that the AgNPs synthesized by the Lee−Meisel method were morphologically diverse, and their sizes varied in a wide range (30−200 nm).

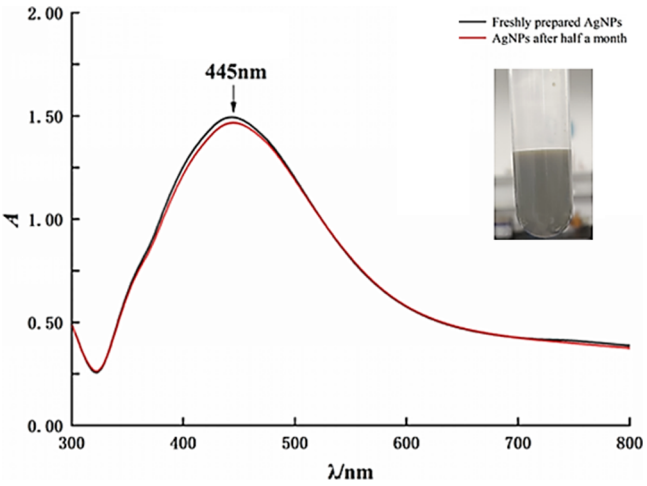

Figure 1. UV−vis spectra of AgNPs. The inset shows a photograph of the AgNP solution.

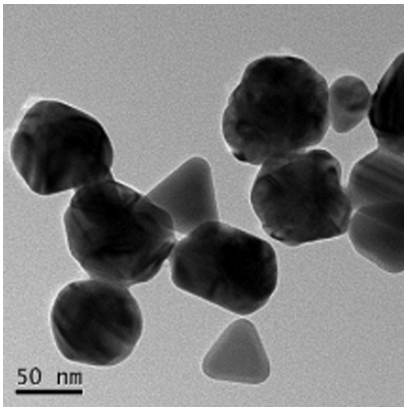

Figure 2. TEM image of AgNPs.

2.3. Characterization of Different Hydrophobic PDMS. Stretching can change the surface roughness of PDMS films, thereby altering their hydrophobicity. The increase in surface roughness allows the surface of hydrophilic substances to become more hydrophilic while that of hydrophobic substances to be more hydrophobic.

According to Figure 3, the greater is the degree of PDMS stretching, the higher is the surface contact angle, indicating the increase in surface hydrophobicity. However, due to the stretch limits of PDMS itself, the fracture will occur when the stretching degree exceeds 150%. Therefore, in the subsequent experimental process, the PDMS at 150% elongation was used.

The contact angle in Figure 4a shows that the stretched shrunk PDMS surface exhibits better hydrophobicity. Therefore, the molecules to be detected are more accumulated on the stretched shrunk PDMS. As seen in Figure 4b,c, the distribution of AgNPs on the stretched shrunk PDMS is not uniform, and more AgNPs will be concentrated in the areas where surface unevenness occurs due to stretching and shrinking.

2.4. Coffee Ring Detection Area. In the next step, 12 μL of 1×10^{-2} mol/L R6G solution mixed with 12 μL of AgNPs solution were dropped on the PDMS surface and subjected to natural drying. A pattern similar to coffee rings appeared on

https://doi.org/10.1021/acsomega.3c00179
ACS Omega 2023, 8, 14541−14548

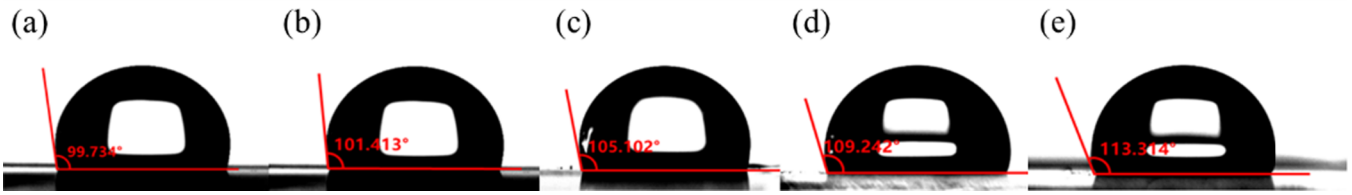

Figure 3. Contact angle images of PDMS at various stretching degrees: (a) 0%, (b) 40%, (c) 80%, (d) 100%, and (e) 150%.

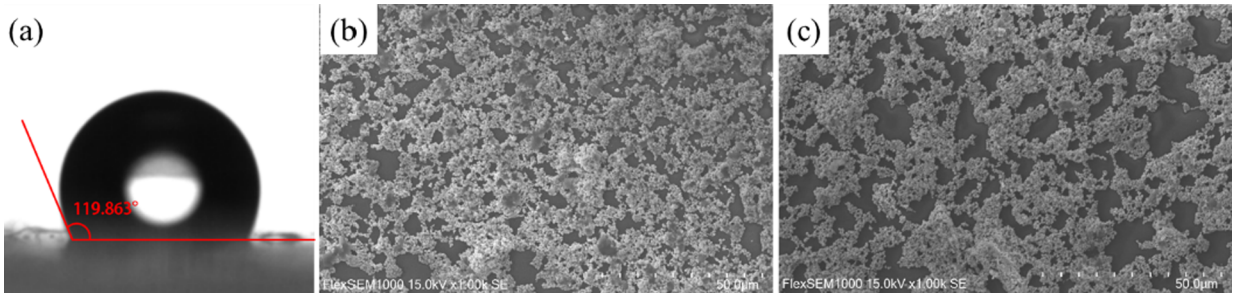

Figure 4. (a) Contact angle image of the stretched shrunk PDMS. SEM images of AgNPs deposited on (b) unstretched PDMS and (c) stretched shrunk PDMS.

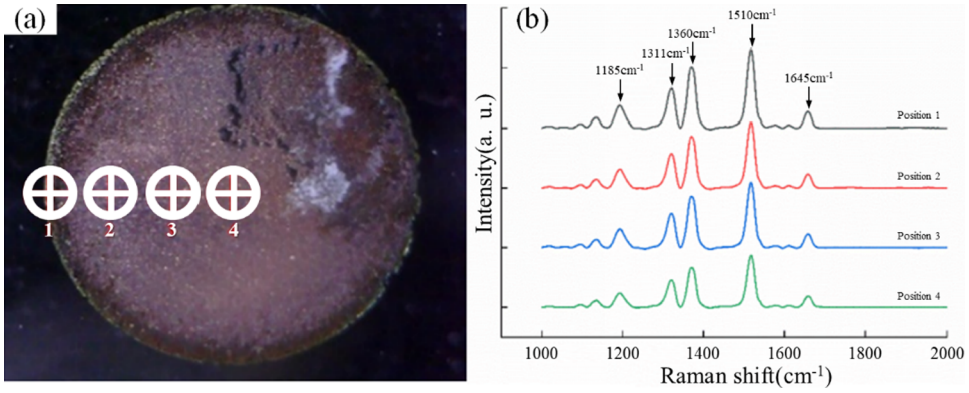

Figure 5. (a) Coffee ring pattern of 1×10^{-2} mol/L R6G solution. Here, 1, 2, 3, and 4 are the SERS analysis regions. (b) Raman spectra of the AgNPs@R6G mixture solution at different points of the coffee ring pattern.

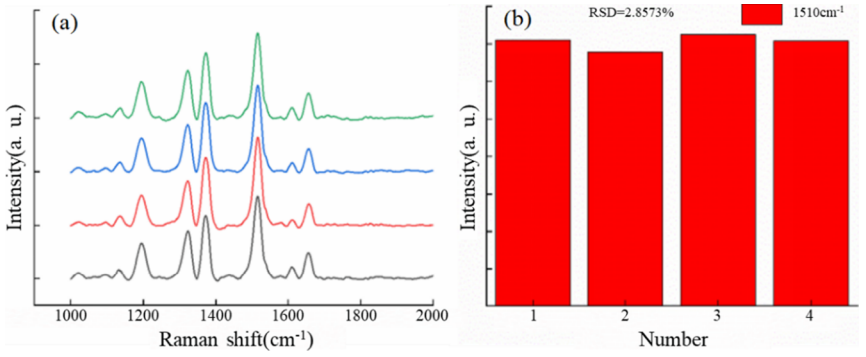

Figure 6. (a) SERS spectra and (b) intensity distribution of the R6G characteristic peak at 1510 cm^{-1} at position 1.

the substrate after drying, as seen in the photograph in Figure 5a, which exhibited a well-defined morphology with obvious ringlike edges. To investigate the relationship between the coffee ring detection region and the Raman signal, four different positions were selected for Raman spectroscopy analysis. Figure 5b displays the SERS spectra acquired at various points. It is evident that the maximum enhancement in the SERS signal was achieved on the edge of the ring, and the intensities of the five characteristic peaks of R6G gradually decreased while moving toward the central region. Therefore, position 1 was the most optimal for the SERS analysis, and the subsequent experiments were performed at this part of the substrate.

2.5. Repeatability of Raman Signals in the Detection Region. To elucidate the detection effect of position 1 on the coffee ring, 1×10^{-2} mol/L R6G solution was used as the

https://doi.org/10.1021/acsomega.3c00179
ACS Omega 2023, 8, 14541−14548

Table 1. Tentative Peak Assignments Representative of R6G SERS Vibrational Modes

standard peak position (cm^{-1})	tentative peak assignment	measure the peak position (cm^{-1})
1187	C−C stretch vibration	1185
1312	C−N stretch vibration on the aromatic ring	1311
1367	C−C stretch vibration on the aromatic ring	1360
1514	C═C stretch vibration on the benzene ring	1510
1662	C═C stretch vibration on the benzene ring	1645

probe molecule. After a coffee ring pattern was formed by the evaporation of the AgNPs@R6G mixed solution, the measurements were repeated four times at position 1 (see Figure 6). In all cases, the characteristic peaks of R6G were identified at 1510 cm^{-1}, and the relative standard deviation (RSD) of the peak intensities was 2.5544%. This result indicated the reproducibility of the Raman signal at position 1.

2.6. Raman Detection of R6G on Different Substrates.

To evaluate the detection sensitivity of different substrates, various concentrations of R6G solutions (10^{-2}−10^{-7} M) were mixed with AgNPs and added dropwise onto the surfaces of the quartz glass sheet, unstretched PDMS surface, stretched unshrunk PDMS surface, and stretched shrunk PDMS surface. After waiting for the formation of coffee-ring patterns by natural evaporation of solutions, the SERS analysis was performed on each substrate. The experiments were done within the wavenumber range of 1000−2000 cm^{-1} at the laser transmitter power of 18 mW, the integration time of 5 s, and the cumulative number of times of 1. The Raman characteristic peaks detected at around 1185, 1311, 1360, 1510, and 1645 cm^{-1} were attributed to R6G solution (Table 1).

The spectra after smoothing are shown in Figure 7, in which the characteristic peaks of 1×10^{-2}, 1×10^{-3}, 1×10^{-4}, 1×10^{-5}, 1×10^{-6}, and 1×10^{-7} M R6G solutions could be clearly distinguished. It is noteworthy that the R6G concentration of 1×10^{-7} M corresponds to a relatively low peak intensity compared to the concentration of 1×10^{-2} M. Moreover, the characteristic peak at the R6G concentration of 1×10^{-7} M was flattened when the spectra at various R6G concentrations

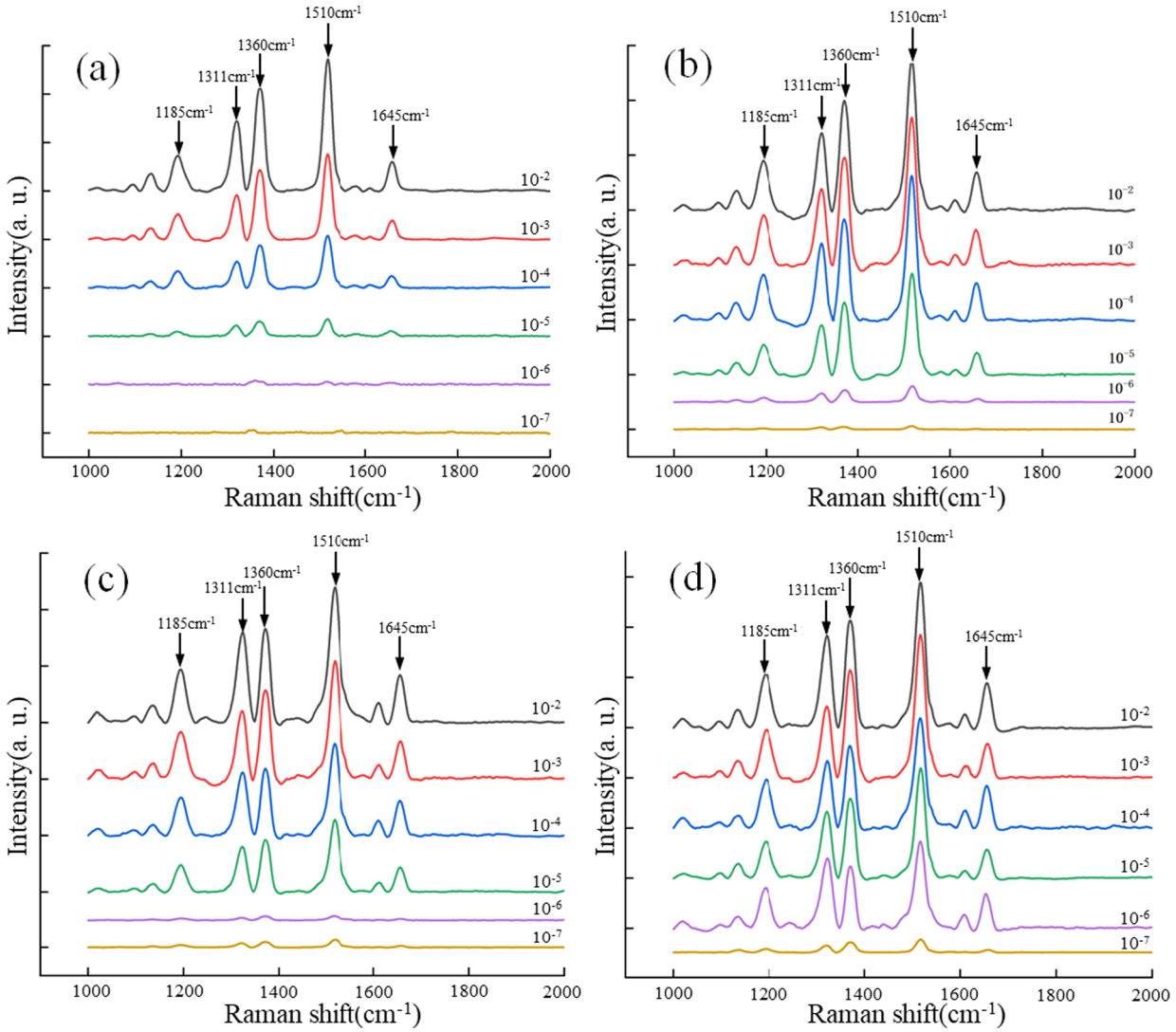

Figure 7. Raman spectra at different AgNPs@R6G concentrations on (a) the quartz glass sheet surface, (b) unstretched PDMS surface, (c) stretched unshrunk PDMS surface, and (d) stretched shrunk PDMS surface.

https://doi.org/10.1021/acsomega.3c00179
ACS Omega 2023, 8, 14541−14548

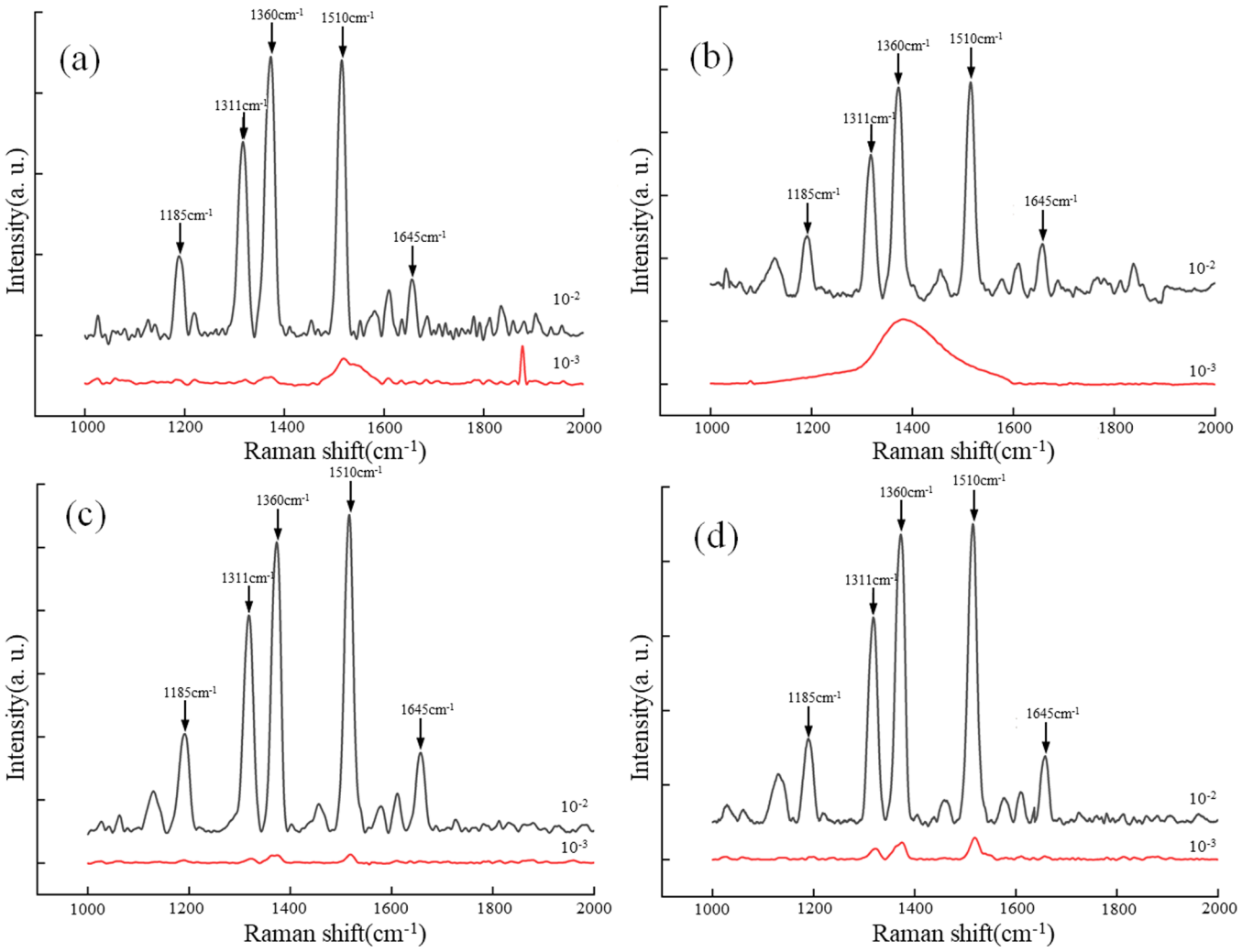

Figure 8. Raman spectra at different concentrations of R6G solution on (a) the quartz glass sheet surface, (b) unstretched PDMS surface, (c) stretched unshrunk PDMS surface, and (d) stretched shrunk PDMS surface.

were displayed as the Y-offset graphs, making the effect less obvious.

Figure 8 depicts the Raman spectra of the AgNPs-free R6G. A prominent feature at 1510 cm^{-1} was ascribed to the characteristic C═C stretching vibration within the benzene ring of R6G.[46] Therefore, this peak was selected for the calculation and comparison of the SERS enhancement factor.[47] Comparing the Raman bands at 1510 cm^{-1} in Figures 7 and 8, the enhancement factors from AgNPs on different substrates were calculated according to eq 1 (see Subsection 4.4 of the Experimental Section) and varied in the descending order as follows: stretched unshrunk PDMS (7.06×10^2) < quartz glass sheet (7.45×10^2) < unstretched PDMS (4.41×10^3) < stretched shrunk PDMS (2.16×10^4).

3. CONCLUSIONS

A stretchable and flexible micro−nano PDMS substrate for rapid detection and identification of organic dyes via SERS was demonstrated. In particular, a wrinkled structure formed on the surface of the PDMS film provided abundant hot spots and pronounced surface hydrophobicity. To investigate the effects of the substrate type and hydrophobicity degree on the Raman signal, different concentrations of R6G were mixed with AgNPs to form the AgNPs@R6G mixed solution, which was then dropped onto various surfaces for SERS detection. The experimental results showed that the best hydrophobicity and Raman enhancement within the stretchable range of PDMS were achieved at 150% elongation. It was also found that the detection of R6G solution was the most accurate when using PDMS after stretching and shrinkage as a substrate. All the characteristic peaks were clearly resolved, indicating that the stretched and shrunk PDMS ensured a significant SERS enhancement. Therefore, this study opens up new prospects for the development of highly efficient stretchable SERS substrates based on flexible materials for detecting various organic dyes in water.

4. EXPERIMENTAL SECTION

4.1. Materials and Instruments. The 785 nm laser and light probe were purchased from Shanghai Ruhai Optoelectronics Technology Co. The grating spectrometer was provided by Beijing Jolyhanguang Instruments Co. A CCD camera was purchased from Andorra Technologies Ltd. UK. A benchtop high-speed centrifuge was produced by Hangzhou Mingyuan Instruments Co. A collector-type thermostatic heating magnetic stirrer was purchased from Gongyi Yuhua Instruments Co. Ultrasonic cleaners were provided by Shenzhen Jiejun Cleaning Equipment Co. A blast drying

https://doi.org/10.1021/acsomega.3c00179
ACS Omega 2023, 8, 14541−14548

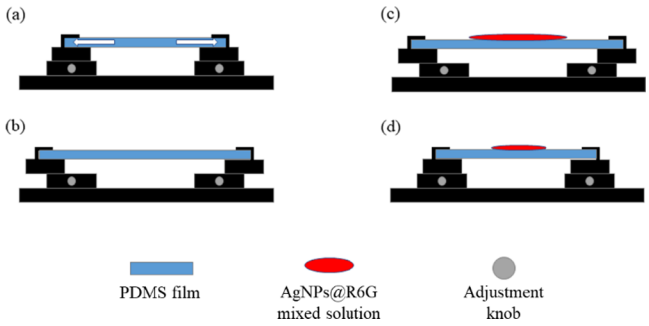

Figure 9. Schematic diagram of PDMS films for SERS detection at different stretching levels. (a) PDMS substrate fixed on a self-made stretcher. (b) PDMS substrate under different degrees of elongation. (c) AgNPs@R6G mixture added dropwise onto the stretched PDMS substrate. (d) AgNPs@R6G mixture shrunk after natural air-drying.

oven was manufactured by Shanghai Jinghong Experimental Equipment Co. An ultraviolet−visible spectrophotometer (UV−vis) was purchased from Shanghai Prism Technology Co. A TEM instrument was purchased from USA Field Electron and Ion Co., Ltd. The micro-regional Raman system and PDMS tensioner were self-made.

4.2. Synthesis of AgNPs. $AgNO_3$ (36 mg) and 200 mL of deionized water were added to a 250 mL three-neck flask and heated to 120 °C in an oil bath. At the same time, 1% sodium citrate solution was prepared for subsequent ultrasonic shaking and mixing, after which 4 mL of the mixed solution was poured into the three-neck flask. The solution was then adjusted to 115 °C and stirred for 1.5 h. As soon as the reaction triggered by heating and stirring stopped, the obtained product exhibited a gray−green color after cooling to room temperature. The product was centrifuged to remove the supernatant and to obtain the highest possible concentration of AgNPs.

4.3. Raman Detection of Organic Dyes in PDMS with Different Stretching Degrees. The PDMS film was clamped onto the stretcher so that the stretching and shrinking of the film were controlled by adjusting the distance between the ends of the stretcher. Then, a drop of the prepared R6G solution of different concentrations (10^{-2}−10^{-7} M) was mixed with AgNPs, and the final mixtures were added dropwise onto the PDMS film under different stretching degrees (0, 40, 80, 100, and 150%). After that, the coffee rings formed by natural evaporation on the substrate surface were subjected to Raman spectroscopy analysis at a laser excitation wavelength of 785 nm. The flow chart of the Raman detection of specific organic dyes on PDMS films with different stretching degrees is shown in Figure 9.[48]

4.4. SERS Enhancement Factor Calculation. The SERS enhancement factor enables one to evaluate the enhancement effect of the SERS substrate according to the equation below:

$$EF = (I_{SERS}/C_{SERS})/(I_{NRS}/C_{NRS}) \quad (1)$$

Here, I_{SERS} and I_{NRS} are the intensities of the enhanced and unenhanced Raman peaks, respectively; C_{SERS} and C_{NRS} are the concentrations of the probe molecule after enhancement and without enhancement, respectively.

AUTHOR INFORMATION

Corresponding Authors

Xuefei Zhang − *School of Material Science and Engineering, Anhui University of Science and Technology, Huainan, Anhui 232001, P. R. China*; Email: zhangxuefeifd@foxmail.com

Changguo Xue − *School of Material Science and Engineering, Anhui University of Science and Technology, Huainan, Anhui 232001, P. R. China*; orcid.org/0000-0001-9671-5542; Email: chgxue@foxmail.com

Authors

Yuanhang Tan − *School of Material Science and Engineering, Anhui University of Science and Technology, Huainan, Anhui 232001, P. R. China*

Kang Yang − *School of Material Science and Engineering, Anhui University of Science and Technology, Huainan, Anhui 232001, P. R. China*

Ziyu Zhou − *School of Material Science and Engineering, Anhui University of Science and Technology, Huainan, Anhui 232001, P. R. China*

Yiting Xu − *School of Material Science and Engineering, Anhui University of Science and Technology, Huainan, Anhui 232001, P. R. China*

Atian Xie − *School of Material Science and Engineering, Anhui University of Science and Technology, Huainan, Anhui 232001, P. R. China*

Complete contact information is available at: https://pubs.acs.org/10.1021/acsomega.3c00179

Notes

The authors declare no competing financial interest.

ACKNOWLEDGMENTS

This work was supported by the National Natural Science Foundation of China (grant nos. 11872001) and the Key Research and Development Program Projects in Anhui Province 2020 (grant nos. 202004h07020026).

REFERENCES

(1) Yang, B. W.; Guo, S.; Jin, S.; Park, E.; Chen, L.; Jung, Y. M. Charge transfer study for semiconductor and semiconductor/ metal composites based on surface-enhanced Raman scattering. *Bull. Korean Chem. Soc.* **2021**, *42*, 1411−1418.

(2) Zhou, C. Y.; Li, H.; Gao, F.; Song, C.; Yang, D.; Xu, F.; Liu, N.; Ke, Y.; Su, S.; Wang, P. Programming Surface-Enhanced Raman Scattering of DNA Origami-templated Metamolecules. *Nano Lett.* **2020**, *20*, 3155−3159.

(3) Kim, J. S.; Cha, S.; Oh, J.; Nam, J. Single-Particle Analysis on Plasmonic Nanogap Systems for Quantitative SERS. *J. Raman Spectrosc.* **2021**, *52*, 375−385.

(4) Huang, Y. F. W.; Guo, H. Y.; Zhan, C.; Duan, S.; Zhan, D.; Wu, D. Y.; Ren, B.; Tian, Z. Q. Microphotoelectrochemical Surface-Enhanced Raman Spectroscopy: Toward Bridging Hot-Electron Transfer with a Molecular Reaction. *J. Am. Chem. Soc.* **2020**, *142*, 8483−8489.

(5) Bell, S. E. J.; Charron, G.; Cortes, E.; Kneipp, J.; De La Chapelle, M. L.; Langer, J.; Prochazka, M.; Tran, V.; Schlucker, S. Towards Reliable and Quantitative Surface-Enhanced Raman Scattering (SERS): From Key Parameters to Good Analytical Practice. *Angew. Chem., Int. Ed. Engl.* **2020**, *59*, 5454−5462.

(6) Albrecht, M. G. C. Anomalously intense Raman spectra of pyridine at a silver electrode. *J. Am. Chem. Soc.* **1977**, *99*, 5215.

(7) Fleischmann, M. P. H.; Mcquillan, A. J. Raman Spectra of Pyridine Adsorbed at a Silver Electrode. *Chem. Phys. Lett.* **1974**, *26*, 163−166.

(8) Kruszewski, S. Dependence of SERS signal on surface roughness. *Surf. Interface Anal.* **1994**, *21*, 830−838.

(9) Liu, G. L. L. Nanowell surface enhanced Raman scattering arrays fabricated by soft-lithography for label-free biomolecular detections in integrated microfluidics. *Appl. Phys. Lett.* **2005**, *87*, No. 074101.

(10) Haynes, C. L.; McFarland, A. D.; Duyne, R. P. V. Surface-enhanced Raman spectroscopy. *Anal. Chem.* **2005**, *77*, 338 A−346 A.
(11) Kneipp, J. K.; Kneipp, K.; Kneipp, K. SERS−a single-molecule and nanoscale tool for bioanalytics. *Chem. Soc. Rev.* **2008**, *37*, 1052−1060.
(12) Cialla, D. M.; Bohme, R.; Theil, F.; Weber, K.; Schmitt, M.; Popp, J. Surface-enhanced Raman spectroscopy (SERS): progress and trends. *Anal. Bioanal. Chem.* **2012**, *403*, 27−54.
(13) Kang, H. Y.; Noh, M. S.; Jo, A.; Jeong, S.; Lee, M.; Lee, S.; Chang, H.; Lee, H.; Jeon, S. J.; Kim, H. I.; Cho, M. H.; Lee, H. Y.; Kim, J. H.; Jeong, D. H.; Lee, Y. S. One-step synthesis of silver nanoshells with bumps for highly sensitive near-IR SERS nanoprobes. *J. Mater. Chem. B* **2014**, *2*, 4415−4421.
(14) Schlücker, S. Surface-Enhanced Raman Spectroscopy: Concepts and Chemical Applications. *Angew. Chem., Int. Ed.* **2014**, *53*, 4756−4795.
(15) Yang, J. K. K.; Lee, H.; Jo, A.; Jeong, S.; Jeon, S. J.; Kim, H. I.; Lee, H. Y.; Jeong, D. H.; Kim, J. H.; Lee, Y. S. Single-step and rapid growth of silver nanoshells as SERS-active nanostructures for label-free detection of pesticides. *ACS Appl. Mater. Interfaces* **2014**, *6*, 12541−12549.
(16) Jun, B. H. K.; Jeong, S.; Noh, M. S.; Pham, X. H.; Kang, H.; Cho, M. H. K.; Lee, Y. S.; Jeong, D. H. Silica core-based surface-enhanced Raman scattering (SERS) tag: Advances in multifunctional sers nanoprobes for bioimaging and targeting of biomarkers. *Bull. Korean Chem. Soc.* **2015**, *36*, 963−978.
(17) Nie, S. E.; Emory, S. R. Probing Single Molecules and Single Nanoparticles by Surface-Enhanced Raman Scattering. *Science* **2018**, *275*, 1102−1106.
(18) Chen, L. C.; Choo, J. Recent advances in surface-enhanced Raman scattering detection technology for microfluidic chips. *Electrophoresis* **2008**, *29*, 1815−1828.
(19) Porter, M. D. L.; Siperko, L. M.; Wang, G.; Narayanan, R. SERS as a bioassay platform: fundamentals, design, and applications. *Chem. Soc. Rev.* **2008**, *37*, 1001−1011.
(20) Lee, M. L.; Kim, K. H.; Oh, K. W.; Choo, J. SERS-based immunoassay using a gold array-embedded gradient microfluidic chip. *Lab Chip* **2012**, *12*, 3720−3727.
(21) Garcia-Rico, E. A.-P.; Guerrini, L. Direct surface-enhanced Raman scattering (SERS) spectroscopy of nucleic acids: from fundamental studies to real-life applications. *Chem. Soc. Rev.* **2018**, *47*, 4909−4923.
(22) Han, Y. Q.; Gao, Y.; Gao, J.; He, Q.; Liu, H.; Han, L.; Zhang, Y. Large-area surface-enhanced Raman spectroscopy substrate by hybrid porous GaN with Au/Ag for breast cancer miRNA detection. *Appl. Surf. Sci.* **2021**, *541*, No. 148456.
(23) Wu, T. Z.; Kou, Y.; Su, X.; Kadasala, N. R.; Gao, M.; Chen, L.; Han, D.; Liu, Y.; Yang, J. Self-sustainable and recyclable ternary Au@Cu(2)O-Ag nanocomposites: application in ultrasensitive SERS detection and highly efficient photocatalysis of organic dyes under visible light. *Microsyst. Nanoeng.* **2021**, *7*, 23.
(24) Liu, J. Z.; Zhang, S.; Yu, H.; Xie, W. A versatile β-cyclodextrin functionalized silver nanoparticle monolayer for capture of methyl orange from complex wastewater. *Chin. Chem. Lett.* **2020**, *31*, 539−542.
(25) Huang, Q. W.; Wei, W.; Yan, Q.; Wu, C.; Zhu, X. A facile and green method for synthesis of reduced graphene oxide/Ag hybrids as efficient surface enhanced Raman scattering platforms. *J. Hazard. Mater.* **2015**, *283*, 123−130.
(26) Pandey, P. V.; Yoon, J.; Kim, B.; Choi, C. S.; Sohn, J. I.; Hong, W. Silver nanowire-network-film-coated soft substrates with wrinkled surfaces for use as stretchable surface enhanced Raman scattering sensors. *J. Alloys Compd.* **2021**, *859*, No. 157862.
(27) Lan, L. G. Y.; Fan, X.; Li, M.; Hao, Q.; Qiu, T. The origin of ultrasensitive SERS sensing beyond plasmonics. *Front. Phys.* **2021**, *16*, 43300.
(28) Xu, K. Z.; Takei, K.; Hong, M. Toward Flexible Surface-Enhanced Raman Scattering (SERS) Sensors for Point-of-Care Diagnostics. *Adv. Sci.* **2019**, *6*, No. 1900925.
(29) Yilmaz, M. B.; Ozdemir, M.; Gieseking, R. L.; Dede, Y.; Tamer, U.; Schatz, G. C.; Facchetti, A.; Usta, H.; Demirel, G. Nanostructured organic semiconductor films for molecular detection with surface-enhanced Raman spectroscopy. *Nat. Mater.* **2017**, *16*, 918−924.
(30) Wang, Y. G.; Wang, S. J.; Yang, X.; Ling, Y.; Yap, L. W.; Dong, D.; Simon, G. P.; Cheng, W. Standing Enokitake-like Nanowire Films for Highly Stretchable Elastronics. *ACS Nano* **2018**, *12*, 9742−9749.
(31) Jiang, T. W.; Tang, J.; Tang, S. Seed-mediated synthesis of floriated Ag nanoplates as surface enhanced Raman scattering substrate for in situ molecular detection. *Mater. Res. Bull.* **2018**, *97*, 201−206.
(32) Wen, J. Z.; Chen, H.; Zhang, W.; Chen, J. Stretchable plasmonic substrate with tunable resonances for surface-enhanced Raman spectroscopy. *J. Opt.* **2015**, *17*, No. 114015.
(33) Zhao, X. Y.; Zhang, C.; Chen, C.; Xu, S.; Li, C.; Li, Z.; Zhang, S.; Liu, A.; Man, B. Flexible and stretchable SERS substrate based on a pyramidal PMMA structure hybridized with graphene oxide assisvated AgNPs. *Appl. Surf. Sci.* **2018**, *455*, 1171−1178.
(34) Yang, Z. W.; Bi, L.; Chen, L.; Wang, G.; Chen, G.; Ye, C.; Pan, J. Wearable electronics for heating and sensing based on a multifunctional PET/silver nanowire/PDMS yarn. *Nanoscale* **2020**, *12*, 16562−16569.
(35) Park, S. L.; Ko, H. Transparent and Flexible Surface-Enhanced Raman Scattering (SERS) Sensors Based on Gold Nanostar Arrays Embedded in Silicon Rubber Film. *ACS Appl. Mater. Interfaces* **2017**, *9*, 44088−44095.
(36) Hatab, N. A. A.; Oran, J. M.; Sepaniak, M. J. Surface-enhanced Raman spectroscopy substrates created via electron beam lithography and nanotransfer printing. *ACS Nano* **2008**, *2*, 377.
(37) Men, D. W.; Wang, C.; Xiang, J.; Yang, G.; Wan, C.; Zhang, H. Wafer-Scale Hierarchical Nanopillar Arrays Based on Au Masks and Reactive Ion Etching for Effective 3D SERS Substrate. *Materials* **2018**, *11*, 239.
(38) Kumar, S. L.; Goel, P.; Neeti; Mishra, P.; Singh, J. P. A facile method for fabrication of buckled PDMS silver nanorod arrays as active 3D SERS cages for bacterial sensing. *Chem. Commun.* **2015**, *51*, 12411−12414.
(39) Zhang, L. L.; Hirata, A.; Chen, M. Wrinkled Nanoporous Gold Films with Ultrahigh Surface-Enhanced Raman Scattering Enhancement. *ACS Nano* **2011**, *5*, 4407−4413.
(40) Yu, Y. N.; Konig, T. A. F.; Fery, A. Tackling the Scalability Challenge in Plasmonics by Wrinkle-Assisted Colloidal Self-Assembly. *Langmuir* **2019**, *35*, 8629−8645.
(41) Xu, K. W.; Tan, C. F.; Kang, N.; Chen, L.; Ren, L.; Thian, E. S.; Ho, G. W.; Ji, R.; Hong, M. Uniaxially Stretched Flexible Surface Plasmon Resonance Film for Versatile Surface Enhanced Raman Scattering Diagnostics. *ACS Appl. Mater. Interfaces* **2017**, *9*, 26341−26349.
(42) Zhang, C. Y.; Yang, N.; Gao, Y.; Jiang, L.; Yin, P. Hydrophobic paper-based SERS platform for direct-droplet quantitative determination of melamine. *Food Chem.* **2019**, *287*, 363−368.
(43) Lee, H. K. L.; Zhang, Q.; Phang, I. Y.; Tan, J. M.; Cui, Y.; Ling, X. Y. Superhydrophobic surface-enhanced Raman scattering platform fabricated by assembly of Ag nanocubes for trace molecular sensing. *ACS Appl. Mater. Interfaces* **2013**, *5*, 11409−11418.
(44) Ma, Y. L.; Chen, Y.; Gu, C.; Wei, G.; Jiang, T. Improved lateral flow strip based on hydrophilic−hydrophobic SERS substrate for ultra−sensitive and quantitative immunoassay. *Appl. Surf. Sci.* **2020**, *529*, No. 147121.
(45) Chen, R. Z.; Li, X.; Ong, L.; Soe, Y. G.; Sinsua, N.; Gras, S. L.; Tabor, R. F.; Wang, X.; Shen, W. Trace Analysis and Chemical Identification on Cellulose Nanofibers-Textured SERS Substrates Using the "Coffee Ring" Effect. *ACS Sens.* **2017**, *2*, 1060−1067.
(46) Song, Y. P.; Long, N. V.; Huang, Z.; Yang, Y. Multifunctional self-assembly 3D Ag/g-C3N4/RGO aerogel as highly efficient adsorbent and photocatalyst for R6G removal from wastewater. *Appl. Surf. Sci.* **2021**, *542*, No. 148584.

https://doi.org/10.1021/acsomega.3c00179
ACS Omega 2023, 8, 14541−14548

(47) Wang, J. L.; Wang, D.; Yu, H.; He, W.; Jiang, W.; Liu, C.; Zhu, E.; Li, H. Synthesis of PVDF membrane loaded with wrinkled Au NPs for sensitive detection of R6G. *Talanta* **2022**, *249*, No. 123676.
(48) Kumar, P. K.; Soni, M.; Deva, D.; Sharma, S. K. A highly sensitive, flexible SERS sensor for malachite green detection based on Ag decorated microstructured PDMS substrate fabricated from Taro leaf as template. *Sens. Actuators, B* **2017**, *246*, 477−486.

https://doi.org/10.1021/acsomega.3c00179
ACS Omega 2023, 8, 14541−14548